Spermatozoa methylome and its sensitivity to water temperature in a teleost fish

Aurélien Brionne, Anne-Sophie Goupil, Stéphanie Kica, Jean-Jacques Lareyre, Catherine Labbé, Audrey Laurent

SPERMATOZOA METHYLOME AND ITS SENSITIVITY TO WATER TEMPERATURE IN A TELEOST FISH

Aurélien Brionne[1], Anne-Sophie Goupil[1], Stéphanie Kica[1], Jean-Jacques Lareyre[1], Catherine Labbé[1] and Audrey Laurent[1*]

[1] INRAE, UR1037 LPGP, Fish Physiology and Genomics, Campus de Beaulieu, F-35000 Rennes, France

[*] corresponding author: audrey.laurent@inrae.fr

ABSTRACT

Global climate change and heat waves are sources of stress which fish are facing in the wild as well as in aquaculture context. In coping with important environmental variations, they demonstrate a great plasticity and a tendency for acclimation throughout generations. Here, we question whether fish might be prone to transmit epigenetic alterations through their gametes to their offspring, thus driving rapid environmental adaptation. The question of epigenetic inheritance in fish has become of crucial interest in the recent years, when the mammalian model of methylome erasure in germ cells and embryos was found not to be conserved. In this work, by sequencing spermatozoa after bisulfite conversion, we characterized the methylation landscape of the paternal gamete in rainbow trout (in comparison to muscle) before to demonstrate its sensitivity to a 4°C increased rearing temperature during spermatogenesis. We found that spermatozoa methylome specifically primes housekeeping and developmental genes for activation and might be instrumental to early development. Most of these methylation-free promoters were not affected by temperature, attesting the robustness of the epigenetic programming of early development. However, the increase of temperature triggered the differential methylation of 5,359 regions, among which 560 gene promoters control spermiogenesis and lipid metabolism. We therefore report, for the first time in fish, that sperm epigenetic landscape carries marks of parental thermal living conditions, suggesting that DNA methylation might be a molecular basis of intergenerational inheritance.

KEY WORDS

Spermatozoa, DNA Methylation, Temperature, Inheritance, Fish

HIGHLIGHTS

- Rainbow trout sperm methylome is sensitive to temperature
- Developmental gene promoters are not affected by a temperature increase
- Spermiogenesis and lipid metabolism gene promoters are modulated by a temperature increase
- Sperm methylome might be a molecular vector of transgenerational acclimation to environmental change

INTRODUCTION

Fish demonstrate a great phenotypic plasticity, which allows them to cope with important environmental variations. At the basis of this plasticity, lies the capacity of the genomes to interact with the environment through epigenetic mechanisms. Epigenetic landscapes indeed regulate cellular transcriptional programs and phenotypes. They rely on DNA methylation and histone post-translational modifications, and are either inherited from a mother cell or modulated upon physiological context.

Increasing evidence indicates that epigenetic information, and *a fortiori* its alteration, are transmittable through meiosis and fertilization, from generation to generation. This is particularly suggested by environmental acclimation studies in fish, where offspring performances were shown to be influenced by the life conditions of their genitors. In the tropical reef fish *Acanthochromis polyacanthus*, the aerobic scope of individuals raised from hatching to adulthood at higher

temperatures (+1.5°C and 3°C) is increased if their parents were also reared at these increased temperatures (Donelson et al., 2012). In the stickleback *Gasterosteus aculeatus*, eggs hatching success and embryo size are influenced by both maternal and paternal exposure to increased temperature (Shama and Wegner, 2014). In the tongue sole *Cynoglossus semilaevis*, thermally-induced sex-reversed pseudo-males have sex-reversed pseudo-male offspring even when these larvae are not exposed to thermal induction (Chen et al., 2014). In the rainbow trout *Oncorhynchus mykiss*, offspring thermotolerance (survival and growth) is improved when genitors also have experienced increased rearing temperature during gametogenesis (Butzge et al., 2021). These data argue in favor of an intergenerational epigenetic inheritance, which suggests that gametes can transmit environmental acclimation clues to the offspring. Very few studies investigated fish gametes epigenetics. So far, Fellous *et al*. reported the differential expression of various epigenetic modifiers in gonads upon increased temperature in stickleback (Fellous et al., 2022), while Gavery *et al.* found in rainbow trout differentially methylated DNA regions in spermatozoa from males of wild versus hatchery origins (Gavery et al., 2018), further indicating that paternal gametes DNA methylome can be modulated by the environment and might be a molecular vector of intergenerational epigenetic inheritance and evolution in fish.

Primarily often neglected, the importance sperm DNA methylome for offspring development was recently demonstrated in zebrafish by a series of studies which revealed that, in contrast to mammalian models, embryo DNA methylome is inherited from spermatozoa, maternal DNA methylome being remodeled before zygotic genome activation to match the paternal one (Jiang et al., 2013; Liu et al., 2018; Potok et al., 2013). In addition, zebrafish do not undergo global DNA methylation reprogramming of primordial germ cells, unraveling the persistence of the epigenetic memory throughout generations (Ortega-Recalde et al., 2019). For a better understanding of the molecular basis underlying fish intergenerational inheritance, data reflecting the full diversity of fish species and reproduction modes are missing, and particularly in the omics perspective.

Given the potential importance of the paternal methylome in fish and in the context of environmental change, we sought to characterize the rainbow trout (*O. mykiss*) sperm methylome and its sensitivity to a water temperature increase. To this aim, we performed whole genome bisulfite sequencing (WGBS) on sperm DNA of trout reared at 12°C or 16°C during gametogenesis. Our strategy included the sequencing of muscle samples from fish raised at 12°C, which was instrumental to identify spermatozoa-specific DNA methylation profiles. We therefore used these single-base resolution data sets to (i) characterize genome-wide methylation dynamics in representative rainbow trout germline and somatic tissues, (ii) highlight the paternal gamete methylome specificities, (iii) assess its sensitivity to a water temperature increase.

RESULTS

Rainbow trout genome features and WGBS datasets

We briefly summarize here the main features of publicly available rainbow trout genome, which are susceptible to impact DNA methylation. *Oncorhynchus mykiss* genome is made of 2.2 Gb parsed into 29 chromosomes with 41,365 and 5,977 coding and non-coding genes, respectively (according to ensembl v105.1 genome annotation of Omyk_1.0 version by Full genebuild). It contains 70,672,452 CpGs (70,671,452 nuclear; 1,118 mitochondrial), with a global genome-wide observed over expected (o/e) CpG ratio of 0.8, indicative of a slight CpG erosion during evolution.

We performed WGBS of sperm (12 °C and 16°C) and muscle (12°C) DNA samples according to the experimental design presented in **Suppl Fig 1**. WGBS yielded a minimum of 300 million paired-end reads of 150bp per sample (**Tab 1**). In all sample types, the average mapping efficiency of the trimmed reads was of approximately 60%. Our final data set contains 65,125,263 CpGs, representing 92% of the trout genome, 70 to 79 % of them being covered at least 5 x. On average, we obtained a sequencing depth of 10-11 x per strand.

We found that almost all methylated cytosines sit in CpG dinucleotides. Indeed, while we measured average methylation of respectively 87.10 and 74.50 % in CpG context in sperm and muscle, respectively, methylated CHG and CHH (H representing A, T or C) were detected at rates lower than 1% (**Suppl Tab 1**). For this reason, this study is dedicated to the analysis of CpG methylation only. Finally, we detected very low CpG methylation on mitochondrial DNA, both in muscle and in spermatozoa (**Tab 1**). Our sequencing depth analysis revealed an important mitochondrial DNA over-representation in muscle *versus* sperm (**Tab 1**). This agrees with the expected differences in ratios of nuclear to mitochondrial DNAs between these tissues with abundant mitochondria in muscle while trout spermatozoa possess a unique semicircular mitochondrion.

Supplementary Table 2 recapitulates, for each sample, the number of cytosines in CpG context, being sequenced as methylated in at least one read. When considering the whole data sets, *circa* 93 % of CpGs, in both tissues, showed at least one positive methylation call. Remarkably, these numbers decreased as the coverage threshold applied to the data increased (5 x; 10 x), and they dropped faster in muscle than in spermatozoa. In fact, among the cytosines covered at least 10 times, 67 % of them, on average, were sequenced as methylated in at least one read in muscle, *versus* 85 % in spermatozoa. This very reproducible observation among fish samples reveals a fragment selection bias in the sequencing library preparation process, likely reflecting differences in the chromatin organization between tissues. Non-methylated DNA fragments are more likely to lie in open and accessible chromatin, more prone to be resuspended in solution and to be represented in the sequencing libraries. Both muscle and spermatozoa WGBS libraries show a better representation of non- or poorly-methylated CpGs, but interestingly, this bias is much milder in spermatozoa, reminiscent of a less heterogeneous chromatin conformation in this cell type.

Rainbow trout genome is globally methylated both in spermatozoa and muscle

To our knowledge, we present the first comprehensive rainbow trout methylomes of somatic and germline representative cell types. We therefore questioned the general trout DNA methylation pattern in a descriptive analysis of sperm and muscle of fish reared in control condition (**Suppl Fig 1, fish 1 to 4**). We first assessed the methylation profile on various genomic features, by calculating the average methylation rates along a reconstituted metagene (**Fig 1A**), around transcription start sites (TSS) and transcription end sites (TES) (**Fig 1B**) of 115,853 annotated Ensembl coding and non-coding transcripts (ensembl v104.1, Omyk_1.0). As already suggested in **Tab 1**, we observed a global DNA hypermethylation of sperm compared to muscle. This result is consistent with the frequently reported high methylation level of spermatozoa in vertebrates (Jiang et al., 2013; Kobayashi et al., 2012; Potok et al., 2013). Nevertheless, both tissues showed a drastic drop of CpG methylation on proximal promoter regions (1kb upstream of TSS) while gene bodies exhibited particularly high methylation rates (**Fig 1 A-B-C**). Repeat elements identified using RepeatMasker (Smit, 2015) were all found to be methylated in both tissues (**Fig 1D**). Transposons, retroposons, LTR, LINEs and SINEs were particularly highly methylated in sperm. Therefore, our analysis of one somatic and one germline tissue showed that, like in most Vertebrates, 5mC in rainbow trout mostly occurs in the CpG dinucleotide context, and shows a global methylation pattern, especially high on gene bodies, and repetitive elements, while gene promoters are more heterogenous and more likely tend to be methylation-free.

The signature of sperm methylation profile reflects spermatogenesis and embryonic development

Seeking for spermatozoa methylome specificities we then ran a comparative analysis of sperm and muscle coupled WGBS data (**Suppl Fig 1B, fish 1 to 4**), from fish reared in control condition. A first approach, by principal component analysis (PCA), led us to observe a clear segregation of sperm and muscle samples in spite of a greater dispersion of muscle samples, likely reflecting the greater complexity of this multicellular tissue compared to sperm (**Fig 2A and Suppl Fig 2**).

Differentially meythylated CpGs (DMCs) between muscle and spermatozoa were identified by DSS (Feng et al., 2014; Wu et al., 2015). We found 36,195,141 DMCs with a threshold adjusted p-value of 0.05, meaning that approximately half of the genome is differentially methylated between muscle and spermatozoa. These DMCs are spread over every chromosome (not shown) and across all genomic features (**Fig 2B, C**). As expected, most of DMCs (98 %) are hypermethylated in sperm compared to muscle. Interestingly, while DMCs hypermethylated in spermatozoa are preferentially found in intergenic regions (also representing the largest part of the genome) (**Fig 2B**), the few sperm-specific hypomethylated DMCs, are significantly enriched in gene bodies and promoters. This is indicative of a structural role of sperm DNA hypermethylation on whole genome chromatin. On the contrary, the enrichment, in spermatozoa, of hypomethylated DMCs in genes and gene-proximal sequences suggests that a few promoters specifically escape the global methylation and might be instrumental for the proper execution of spermatogenic transcriptional program. In order to gain insight into this spermatozoon-specific transcriptional regulation, we isolated promoters and compared their methylation levels in both tissues. Promoter methylation status is indeed informative of a transcriptionally repressed or permissive state (however still sensitive to histone post-translational modifications).

Common hyper-methylated promoters (53862 transcripts, **Fig 3A**, orange rectangle, **Suppl Tab 3A**) were particularly enriched in GO terms referring to cellular transport, cell adhesion and migration, signaling, response to stimulus, homeostasis, metabolism and terminal differentiation (angiogenesis, pulmonary valve differentiation, melanocyte differentiation).

On the other side, 34,925 common hypo-methylated promoters (**Fig 3A**, blue square, **Suppl Tab 3B**) were strongly enriched in GO annotations referring to development (morphogenesis, axis specification, organ development and cell differentiation), germline and housekeeping functions (transcription, translation, metabolism, DNA repair, cell cycle, proliferation, etc). Some signaling, response to stimulus and transport terms also appeared enriched in this category. These data reveal

that many genes supporting early development or housekeeping functions are by default in a permissive state for transcription. Even genes which are not necessarily required in the non-proliferative spermatozoa can nevertheless be primed for transcription in order to support embryo development. As an example, TSS region of *pola2*, a gene that encodes a subunit of the DNA polymerase, is equally hypomethylated in both tissues (**Fig 3B**). A vast majority of transcription factors instrumental for development (*otx*, *cbx* or *pax* families) also have constitutively hypo- or low-methylated promoters, even though they are not constitutively expressed. Their expression levels might be regulated by additional post-translational histone modifications as cells differentiate or face particular contexts.

Spermatozoa-specific hypo-methylated promoters belonging to 861 transcripts (**Fig 3A**, green shape, **Suppl Tab 3C**) were enriched in spermatozoa specific terms such as meiosis and germline, in addition to development, cellular metabolism and IGF signaling. Some of them are markers of the germline, such as *piwil1* involved in transposable elements silencing during gametogenesis, *dazl* which encodes a master translational regulator during spermatogenesis or the sex determining gene *dmrt1* (**Fig 3B**). Others, such as s*po11* or *mei4* encode specific meiotic recombination factors (**Fig 3B**). We also found the promoters of the pluripotency factors encoding *klf4* (**Fig 3B**) and *esrrb* to be specifically hypomethylated. Noticeably, a subset of developmental factors escapes constitutive hypomethylation and is specifically reprogrammed to be hypomethylated in the spermatozoa. This is the case of the entire *hox* clusters (**Fig 3B**), in which remarkably, altogether promoters: gene bodies and intergenic regions, spanning hundreds of kilobases are fully demethylated. The conserved *mir10b*, lying in the vicinity of *hox4* paralogs and co-expressed during development is therefore hypo-methylated as well. Interestingly *meis1a* (**Fig 3B**) or *meis3*, which are *hox* cofactors involved in axis patterning and organ morphogenesis, are also specifically hypomethylated in the spermatozoa. This set of spermatozoa-specific genes is then silenced by methylation in the adult differentiated muscle, meaning that they might be sensitive to a dynamic regulation by promoter methylation.

Finally, 632 muscle-specific hypo-methylated promoters (**Fig 3A**, red shape, **Suppl Tab 3D**) were enriched in terms referring to terminal differentiation, muscle and vasculature function, cellular metabolism, response to stimulus and immune response. These dynamic promoters have undergone a demethylation during differentiation and are likely to be controlling muscle function. They mainly regulate terminal differentiation genes, such as *plecb* encoding a skeletal muscle plectin or signaling molecules such as *rarg* encoding a retinoic acid receptor (**Fig 3B**).

Altogether this work strongly supports the idea that sperm methylome is carrying an epigenetic program, which might be instrumental for both spermatogenesis and proper embryo development.

Increasing rearing temperature alters sperm methylome

Given the importance of the paternal methylome in fish, we sought to question its robustness or sensitivity to environmental conditions. We chose to evaluate the potential impact of an increased rearing water temperature during gametogenesis on rainbow trout spermatozoa methylome. To this aim, we analyzed by WGBS the sperm of 6 fish bred at 16°C from May to November versus 6 control fish kept at 12°C (**Tab 1, Suppl Fig 1B**). Global average methylation rates were similar in both conditions (**Suppl Tab 1**) and the PCA analysis did not show any strong segregation between 12°C and 16°C spermatozoa samples (**Fig 4A and Suppl Fig 2**). Nevertheless, we identified 112,386 DMCs with a threshold adjusted p-value of 0.05 (**Fig 4B**). Nearly 50% of DMCs were hypomethylated (55,738) and 50% hypermethylated (56,648) at 16°C compared to 12°C. Interestingly, we found that 92% of these DMCs fall into differentially methylated regions (DMRs). This result indicates that an increase of rearing water temperature during gametogenesis alters spermatozoa methylome in a non-sporadic and non-random way. The affected cytosines instead concentrate into 5,359 DMRs of 400 bp median length resulting from a coordinated response to temperature increase. Ten % of these DMRs affect promoters, later on designed as prom-DMRs. Noteworthy, very few of these differentially methylated promoters had been previously identified as tissue specific, i.e. hypomethylated exclusively in either

spermatozoa or muscle (11 and 7, respectively) (**Fig 5A**). On the contrary, they mostly fall in the common hypo-, common hyper- or common moderately-methylated promoter categories, already indicating that developmental genes epigenetically reprogrammed in the spermatozoa were mostly unaffected.

In order to thoroughly study the biological functions of the differentially methylated promoters (prom-DMRs), we carried out both (i) a non-biased search for GO terms enrichment, (ii) a manual examination and annotation of the TOP 200 differentially methylated ones. Both approaches were mainly based on gene orthologies and mammalian literature. Examples of hypo- and hyper-methylated gene promoters and enriched GO categories are indicated in **Fig 5A**, **Suppl Tab 4 A-B** and **Suppl Tab 5**. Interestingly, the manual annotation analysis largely confirmed the GO term enrichment test and indicated that the prom-DMRs impacted spermiogenesis and lipid metabolism genes, leaving most developmental genes unaffected.

Intracellular vesicle trafficking

We found prom-DMRs annotations covering virtually the whole spectrum of the molecular components regulating vesicular trafficking and/or autophagy: from plasma and organelle membrane regulation to motor proteins and signaling (**Fig 5A**, **Suppl Tab 5**). We found DMRs in the promoters of *asah2* (N-AcylSphingosine AmidoHydrolase) (**Fig 5B**), *ppm1la* and *cert1* (ceramide transporters), *sphk1* (sphingosine kinase) and *mdga1* (MAM Domain containing Glycosylphosphatidylinositol Anchor), which regulate membrane ceramid and sphingolipid metabolism, therefore affecting membrane properties, lipid rafts, protein sorting, signaling, plasma membrane curvature and endocytosis initiation (Pepperl et al., 2013; Tani et al., 2007; Young and Wang, 2018). The promoter of the membrane receptor *s1pr3* (protein-G-coupled receptor of Phospho-Sphingosine) is differentially methylated as well as the promoters of *vldlr* and *mesd* (very low density lipoprotein receptor and chaperone for low density lipoprotein receptors (LRP), respectively), likely affecting endocytosis

initiation. We found several promoters of signaling molecules regulating vesicular traffic such as *grb2b*, *praf2* and *sh3gl1b* (adaptors), *rab1b* and *rnd2* (small GTPases), *dennd5a*, *rgl2*, *arhgef18a*, *quo*, *fgd4b* and *trappc13* (GEF, guanine nucleotide exchange factors for small GTPases), and *git2a*, *tbc1d2* and *rgs3b* (GAP, GTPases activating proteins). DMRs also affected promoters of vesicular traffic effectors such as the motor myosin *myo5b* (**Fig 5B**), the actin interacting WASP family member *wasf3a* and the kinesin *kif26ba*. Finally, we found prom-DMRs potentially affecting the regulation of membrane fusion, such as the promoters of *nsfl1c* (*p47* ortholog) and *nsfb* (*nsf* ortholog) (**Fig 5B**) encoding representative actors of the two major membrane fusion pathways (NSF and VCP/p47 pathways) (Brunger and DeLaBarre, 2003), the promoter of *rnf126* (E3 ubiquitin ligase, which is essential for proteasomal degradation in the VCP/p47 pathway) (**Fig 5B**), or the promoter of *myofl* involved in membrane fusion and repair. Markers of various types of intracellular vesicles where found differentially methylated, such as *ap5b1* and *ap5s1*, encoding two subunits of the late endosome AP-5 adaptor complex, *trappc13* encoding a component of the trafficking particle protein complex and *vmp1* (vacuole membrane protein), both involved in secretion and autophagy, therefore suggesting that several pathways orchestrating cellular trafficking might be elicited in response to increased rearing temperature. Therefore, sperm cells exposed to increased temperature exhibit a differential methylation at numerous promoters regulating vesicular trafficking potentially involving protein folding and degradation, cell signaling, autophagy or apoptosis.

Cytoskeleton remodeling

We found abundant prom-DMRs indicative of a reorganization of the cytoskeleton, mostly affecting actin network, cell-cell and cell-extra cellular matrix (ECM) adhesion (**Fig 5A**, **Suppl Tab 5**). As such, we found promoters of genes controlling actin dynamics: *flna* (filamin a) (**Fig 5B**), *tmod1* (tropomodulin) (**Fig 5B**), *add2* (adducin), *coro1b* (coronin) and *prkd4* (kinase) (**Fig 5B**), are all reported to interact with actin network and/or control its assembly, filament elongation or depolymerization. In addition,

sema4gb, encoding a semaphorin was found among the prom-DMRs (**Fig 5B**). Semaphorins regulate intra-cellular actin filaments and microtubule network interactions with the ECM. Interestingly, in the same pathway, the promoters of the semaphorin receptors *plkdc2* (plexin) and *nrp1a* (neurpilin) and its co-factor *rftn2* (raftlin) were also differentially methylated. Other promoters of genes encoding components of cellular junctions or cell-ECM adhesion complexes were found among DMRs, such as the protocadherins *pcdh1g32* and *pcdhb*, and the cadherin interacting angiomotin-like *amotl2a* (adherens junctions)*, nectin1a* (adherens junctions), the claudin encoding *cldnd* and *cldn23a* (tight junctions). Finally, other prom-DMRs were reported in the literature to be regulators of cell-cell and cell-ECM adhesion, such as *susd2*, *mpp3b*, *sh3bgrl*, *tbc1d2*, *mdga2a*, *cadm1b* and *rxylt1*. These results highlight a high occurrence of genes related to actin cytoskeleton remodeling, cell-cell and cell-ECM adhesion, among promoters affected by an increased temperature in spermatozoa. This suggests a potential response of differentiating germ cells at the level of both intra- and inter-cellular processes.

Therefore, numerous prom-DMRs annotations converge toward a functional adaptation of germ cells to a temperature stress with a coordinated cytoskeletal reorganization supporting an important modulation of intracellular vesicular trafficking and autophagy. This could be interpreted as a conserved and generic cytoprotective response to heat stress. Similar results were indeed reported by Madeira *et al.* who observed that larvae of sea bream *Sparus aurata* modulate, at the protein level, the intracellular transport, protein folding and degradation and the cytoskeleton dynamics pathways in response to temperature stress (Madeira et al., 2016). Indications of cytoskeleton remodeling in adaptation to increased temperature were also observed in a blue mussel gills (Fields et al., 2012) or in the myofibril tissue of the crab *P. cinctipes* (Garland et al., 2015). During their progression, male germ cells in rainbow trout thus modulate promoters classically involved in somatic heat stress adaptation and keep traces of these alterations in the terminally differentiated spermatozoa.

Spermiogenesis

Beyond the activation of possibly pan cell type adaptive mechanisms to increased rearing temperature, the cellular trafficking and cytoskeleton actors differentially methylated in our study interestingly pinpoint one major function precluding the spermatozoon stage: spermiogenesis. In the testis, differentiating sperm cells undergo drastic cell shape and cell-cell adhesion remodeling. These processes result from a tight control of the cytoskeleton dynamics and a recycling of intercellular junctions and ECM-interacting receptors at the plasma membrane, processes which are in turn dependent on endocytosis, vesicle trafficking, autophagy and protein recycling. Indeed, proper Golgi orientation, cytoskeleton, membrane fusion and vesicular trafficking are essential for the formation of the acrosome. Rainbow trout spermatozoa possess a transitory pseudo-acrosomal vesicle which is visible at the round spermatid stage and only leaves a cytoskeletal scar at later stages, reminiscent of mammalian acroplaxome (Billard, 1983). Endocytosis and vesicle trafficking are also crucial to the intraflagellar vesicle transport of molecules allowing the growth of the flagellum, and later on, for the elimination of the cytoplasm in late spermiogenesis and the individualization of sperm cells from the syncytium for spermiation. These spermiogenetic processes might recruit and coordinate common actors of vesicular trafficking expressed during spermiogenesis. It is therefore tempting to speculate that several gene promoters instrumental for spermiogenesis have been targeted by differential methylation. Interestingly, we found *tmf1* in the list of differentially methylated promoters (**Fig 5B**). Its mouse ortholog TMF/ARA160 encodes a protein associated to Golgi, emerging vesicles and microtubule network, which KO in male germ cells induces Golgi misorientation, lack of homing of pro-acrosomal vesicles, agenesis of the acrosome, inefficient cytoplasm removal and misshapen sperm head (Elkis et al., 2015; Lerer-Goldshtein et al., 2010). Myosin VI and Myosin Va, orthologs of *myo5b*, which we found differentially methylated in our data set, are essential for acrosome formation in the mouse and in the Chinese mitten crab (*E. sinensis*), respectively (Sun et al., 2010; Zakrzewski et al., 2020). The small GTPase *rnd2* mentioned earlier ("intracellular vesicle trafficking section") was detected in Golgi and pro-acrosomal vesicles of rat spermatids (Naud et al., 2003).

In addition, several promoters of genes specifically implicated in other aspects spermatogenesis were found differentially methylated. As such, *rad51ap1* (**Fig 5B**), *rec8b* and *rmi2* (**Fig 5B**) encode essential actors of the meiotic homologous recombination (Bommi et al., 2019; Dray et al., 2011; Pires et al., 2017; Velkova et al., 2021), *aurka* encodes the aurora A kinase, involved in centrosome maturation and spindle formation during mitosis and also found to be essential for meiosis and spermiogenesis in mice (Lester et al., 2021), and *mief* (**Fig 5B**) encodes in human a mitochondrial fusion factor (Zhao et al., 2011), reminiscent of the mitochondrial remodeling to which rainbow trout spermatozoa are subjected during their differentiation. Interestingly, while autophagy is involved in spermiogenesis, and in particular in acrosome formation in mice (Wang et al., 2014), its increase in the human pathological model of cryptorchidism is associated to an impairment of spermatozoa maturation (Yefimova et al., 2019). Remarkably, in spite of the wide variation in spermatozoa morphologies and action modes among animals, cytoskeleton remodeling, vesicle trafficking and autophagy seem to be part of common pathways regulating normal, adaptive or pathological male germ cell maturation (White-Cooper and Bausek, 2010). Prom-DMRs which we detected in our experimental contrast are enriched in these GO categories. Altogether, these results argue in favor of an altered regulation of the late spermatogenic program (meiotic and post-meiotic) upon increased temperature. This could suggest that regions of the genome which were active during the exposure of the fish to the temperature stress (orchestrating late spermatogenesis) were more particularly prone to undergo a modulation of their methylation level.

Lipid metabolism

Interestingly, a third category of abundant prom-DMR annotations relates to the regulation of lipid metabolism (**Fig 5A**, **Suppl Tab 5**). We found several promoters of lipid catabolism genes such as *asah2* (ceramidase), *daglb* (lipase) or *abcd3a* (encoding a transporter involved in peroxisomal transport or catabolism of very long chain fatty acids). The regulation of long chain fatty acid metabolism was more

specifically affected with the differential promoter methylation of *cox-1* (cyclooxygenase involved in arachidonic acid conversion) (**Fig 5B**), *ptges* (terminal enzyme of the cox-2-mediated prostaglandin E2 biosynthesis from arachidonic acid), *gstp1* (glutathione S-transferase), *gpx1* (glutathione peroxidase) and *elovl7b* (fatty acid elongase) (**Fig 5B**). In addition, the promoter of *gps2* (**Fig 5B**), which encodes a PPARɣ transcriptional co-activator, was found differentially methylated. Fatty acid composition in testis was shown to be of particular relevance for sperm maturation and function in human (Collodel et al., 2020), in ruminant (Van Tran et al., 2017), or rooster (Teymouri Zadeh et al., 2020). PPARɣ, known to be master regulator of adipocyte differentiation and lipid metabolism, was also shown to control fatty acid metabolism in human and therefore suspected to be instrumental for proper sperm formation (Olia Bagheri et al., 2021). Finally, the promoter of *hnf4a*, which controls fatty acid oxidation and metabolism in hepatocytes, was overlapping with a DMR in our analysis (**Fig 5B**). The appearance of fatty acid metabolism as a potentially altered pathway, controlled by PPARɣ and/or Hnf4a, could be interpreted as a metabolic adaptation of poikilotherm fish to temperature. The activity of several desaturases, elongases and fatty acid composition where indeed shown to be sensitive to temperature in fish and rainbow trout in particular (Tocher et al., 2004). It is remarkable however to find its scar in the methylation profile or spermatozoa.

CONCLUSION

In the present study, we aimed at characterizing the rainbow trout sperm methylome (using muscle as a somatic reference tissue) and its sensitivity to a rearing temperature increase of 4°C during spermatogenesis. Single-base resolution methylomes revealed that an important pool of gene promoters is methylation-free in spermatozoa, and therefore in a permissive state for transcription, although sperm DNA is tightly packed and transcriptionally silent. Sperm cells thus carry an epigenetic code seemingly resulting from history and preparing their future role. Remarkably, sperm methylation-free promoters control housekeeping, early development and germline functions.

We found that an increased rearing temperature during spermatogenesis significantly impacted sperm methylome. Interestingly, DMRs affected promoters controlling spermiogenesis and lipid metabolism genes, leaving most developmental genes unaffected. This organized response to heat stress suggests a coordination by a signaling pathway. Our data highlighted PPARɣ and Hnf4 pathways. Alternatively, some genomic regions might be more prone to undergo methylome alterations because of a pre-established sensitivity, laying in the fact that they are active during spermiogenesis, which is both a period of deep chromatin remodeling and the time of experimental stress exposure. In an attempt to identify a potential driver of the differential methylation we observed, we looked for enriched transcription factor biding sites (TFBS) in our DMR using MEME suite. Interestingly, the most significantly enriched TFBS was the one of PRDM9 (**Suppl Fig 3**), which binds to recombination hotspots during meiosis. This opens the seducing possibility that meiotic recombination sites are at particular risk of epigenetic reprogramming upon environmental stress. Taken together, for the first time in rainbow trout, our results demonstrate that the methylation status of sperm-specific gene promoters controlling housekeeping and developmental function is very robust in the context of a 4°C temperature increase during spermatogenesis. Remarkably however, we found that the sperm methylome is altered and carry the traces of the life history of the individuals. We found epigenetic alterations of spermiogenesis and lipid metabolism controlling genes, which will be transmitted to the next generation. Future investigation should answer whether this altered sperm epigenome could be a molecular basis of acclimation to a heat stress for next generations and whether it could impact positively or negatively offspring performances under various conditions.

MATERIAL AND METHODS

Ethics statements

The experiment was conducted following the Guidelines of the National Legislation on Animal Care of the French Ministry of Research (Decree No 2013–118, February 2013) and in accordance with EU legal frameworks related to the protection of animals used for scientific purposes (i.e., Directive 2010/63/EU). The scientists in charge of the experiments received training and personal authorization. The experiment was conducted at the INRAE Physiology and Genomic Laboratory (LPGP) experimental facilities (permit number C35-238-6, Rennes, France), and approved by the ethics committee for the animal experimentation of Rennes under the authorization number T-2019-05-AL.

Fish rearing and sampling

Oncorhynchus mykiss rainbow trouts, from a winter spawning strain (December 15 – January 15), were reared in our experimental farm (river water, in which temperatures are near 7.5°C in winter and can reach 20°C in summer). Two groups of 20 males were transferred to our indoor fish facility in April (April 4th 2019) of their second year, when they reached 15 months of age. They were kept in a recycling system, under artificial spring/summer/autumn photoperiod, and at the temperatures of 12°C and 16°C (after 2 weeks acclimation and gradual temperature increase, from April 18th 2019 till sample collection). Regarding the reproductive cycle, this period of experimental exposure corresponds to the post-meiotic phase. For each experimental group, fish were split into two water tanks (10 fish per tank). The growth of the fish in both groups was recorded and their commercial diet rations were adapted so that both groups follow similar growth curves (Supplementary Figure 4). Fish were checked every two weeks for milt production, at the occasion of the measure of their individual weight. Sperms were harvested by stripping (first spermiation) and muscle samples were taken after euthanasia (tricaine 200 mg/mL).

Whole genome bisulfite sequencing

We analyzed by WGBS and compared (i) the sperm of 4 fish bred at 12°C *versus* the muscle of the same 4 fish (reared in control condition), and (ii) the sperm of 6 fish bred at 16 °C from mid-April to November *versus* 6 control fish kept at 12°C (**Tab 1, Suppl Fig 1B**). Genomic DNA was prepared after an overnight lysis in TNES/Urea buffer (10 mM Tris, 0.125 M NaCl, 10 mM EDTA, 17 mM SDS, 4M urea, pH 8) complemented with 80ug/mL proteinase K at 42°C. After phenol-chloroform extraction, the samples were treated with RNase A (4mg/mL) and gDNAs were precipitated by the addition of isopropanol and sodium acetate. Whole genome bisulfite sequencing libraries were prepared (according to Accel-NGS Methyl-Seq DNA library Kit for Illumina protocol, Swift Biosciences) and sequenced in 150 bp paired-end reads by Novogene company.

Bio-informatic analysis

WGBS yielded a minimum of 300 million paired-end 150 bp reads per sample (Tab 1). Quality and adapter trimming of the reads was carried out using Trim Galore (with an additional 10 bp clipping for read2 5'-end and read1 3'-end) (Krueger and Galore, n.d.). After trimming, only uniquely mapped reads on the *O. mykiss* genome or its *in silico* bisulfite converted version were kept for further analysis (using Bismark bio-informatic software and Omyk_1.0 genome version, (Krueger and Andrews, 2011).. BigWig files were obtained with bedGraphToBigWig (Kent et al., 2010) and methylation values were visualized with Integrative Genome Viewer (Robinson et al., 2011). These steps were included in a workflow which agrees to FAIR principles and is accessible online (https://forgemia.inra.fr/lpgp/methylome). The methylome (v1.0) workflow was built in Nexflow dsl2 language using a singularity container and optimized in terms of computing resources (cpu, memory) for its use on an informatic farm with a slurm scheduler.

Differentially methylated cytosines (DMCs) were identified by the R package DSS (Feng et al., 2014; Wu et al., 2015), using the optional methylation level smoothing on 500 bp and a Benjamini-Hochberg adjusted p-value threshold of 0.05. Differentially methylated regions (DMRs) were defined using DSS package with seed regions containing at least 5 CpGs and expansion window criterias agreeing with a minimum of 75 % of DMCs (with raw pval < 0.01).

CpGs were annotated with GenomeFeatures (Brionne, n.d.), RepeatMasker (Smit, 2015) and ensembl v105.1 annotation. Biological interpretations were carried out using ViSEAGO R package (Brionne et al., 2019) and the Gene Ontology (GO) public database. Associated gene terms were implemented from the extended Ensembl Compara custom annotation based on the release 103. Enrichment tests were performed using exact Fisher's test. Enriched GO terms (p-val < 0.01) were grouped into functional clusters by Wang's semantic similarity respecting GO graph topology and Ward's criterion.

AVAILABILITY OF DATA

The data that support the findings are already deposited and will be available on the ENA archive (https://www.ebi.ac.uk/ena/browser/home) under the accession number (PRJEB56697) and following an embargo from the date of publication. They can be transferred to the reviewers upon editor request.

ACKNOWLEDGEMENTS

The study was funded by the department of animal physiology (PHASE) of INRAE (ACI 2019). We thank Julien Bobe for its contribution to the experimental design and his comments on the manuscript. We thank the staff of our experimental farm (PEIMA, INRAE) and fish facility (ISC LPGP) and particularly Cécile Duret for dedicated handling of our experimental fish.

AUTHORS CONTRIBUTIONS STATEMENT

AL designed the project and experiments, supervised the study and wrote the manuscript. CL and JJL contributed to the design of the project. ASG, SK and CL performed the wet lab work. AB performed the bio-informatic analysis. All the authors read and approved the manuscript.

REFERENCES

Billard, R., 1983. Spermiogenesis in the rainbow trout (Salmo gairdneri). An ultrastructural study. Cell Tissue Res. 233, 265–284. https://doi.org/10.1007/BF00238295

Bommi, J.R., Rao, H.B.D.P., Challa, K., Higashide, M., Shinmyozu, K., Nakayama, J.-I., Shinohara, M., Shinohara, A., 2019. Meiosis-specific cohesin component, Rec8, promotes the localization of Mps3 SUN domain protein on the nuclear envelope. Genes Cells Devoted Mol. Cell. Mech. 24, 94–106. https://doi.org/10.1111/gtc.12653

Brionne, A., n.d. GenomeFeatures: A convenient tool for multiple genomic features annotations.

Brionne, A., Juanchich, A., Hennequet-Antier, C., 2019. ViSEAGO: a Bioconductor package for clustering biological functions using Gene Ontology and semantic similarity. BioData Min 12, 16.

Brunger, A.T., DeLaBarre, B., 2003. NSF and p97/VCP: similar at first, different at last. FEBS Lett. 555, 126–133. https://doi.org/10.1016/s0014-5793(03)01107-4

Butzge, A.J., Yoshinaga, T.T., Acosta, O.D.M., Fernandino, J.I., Sanches, E.A., Tabata, Y.A., de Oliveira, C., Takahashi, N.S., Hattori, R.S., 2021. Early warming stress on rainbow trout juveniles impairs male reproduction but contrastingly elicits intergenerational thermotolerance. Sci. Rep. 11, 17053. https://doi.org/10.1038/s41598-021-96514-1

Chen, S., Zhang, G., Shao, C., Huang, Q., Liu, G., Zhang, P., Song, W., An, N., Chalopin, D., Volff, J.-N., Hong, Y., Li, Q., Sha, Z., Zhou, H., Xie, M., Yu, Q., Liu, Y., Xiang, H., Wang, N., Wu, K., Yang, C., Zhou, Q., Liao, X., Yang, L., Hu, Q., Zhang, Jilin, Meng, L., Jin, L., Tian, Y., Lian, J., Yang, J., Miao, G., Liu, S., Liang, Z., Yan, F., Li, Y., Sun, B., Zhang, H., Zhang, Jing, Zhu, Y., Du, M., Zhao, Y., Schartl, M., Tang, Q., Wang, J., 2014. Whole-genome sequence of a flatfish provides insights into ZW sex chromosome evolution and adaptation to a benthic lifestyle. Nat. Genet. 46, 253–260. https://doi.org/10.1038/ng.2890

Collodel, G., Castellini, C., Lee, J.C.-Y., Signorini, C., 2020. Relevance of Fatty Acids to Sperm Maturation and Quality. Oxid. Med. Cell. Longev. 2020, 7038124. https://doi.org/10.1155/2020/7038124

Donelson, J.M., Munday, P.L., McCormick, M.I., Pitcher, C.R., 2012. Rapid transgenerational acclimation of a tropical reef fish to climate change. Nat. Clim. Change 2, 30–32. https://doi.org/10.1038/nclimate1323

Dray, E., Dunlop, M.H., Kauppi, L., San Filippo, J., Wiese, C., Tsai, M.-S., Begovic, S., Schild, D., Jasin, M., Keeney, S., Sung, P., 2011. Molecular basis for enhancement of the meiotic DMC1 recombinase by RAD51 associated protein 1 (RAD51AP1). Proc. Natl. Acad. Sci. U. S. A. 108, 3560–3565. https://doi.org/10.1073/pnas.1016454108

503 Elkis, Y., Bel, S., Rahimi, R., Lerer-Goldstein, T., Levin-Zaidman, S., Babushkin, T., Shpungin, S., Nir, U.,
504 2015. TMF/ARA160 Governs the Dynamic Spatial Orientation of the Golgi Apparatus during
505 Sperm Development. PloS One 10, e0145277. https://doi.org/10.1371/journal.pone.0145277
506 Fellous, A., Wegner, K.M., John, U., Mark, F.C., Shama, L.N.S., 2022. Windows of opportunity: Ocean
507 warming shapes temperature-sensitive epigenetic reprogramming and gene expression
508 across gametogenesis and embryogenesis in marine stickleback. Glob. Change Biol. 28, 54–
509 71. https://doi.org/10.1111/gcb.15942
510 Feng, H., Conneely, K.N., Wu, H., 2014. A Bayesian hierarchical model to detect differentially
511 methylated loci from single nucleotide resolution sequencing data. Nucleic Acids Res 42, e69.
512 Fields, P.A., Zuzow, M.J., Tomanek, L., 2012. Proteomic responses of blue mussel (Mytilus) congeners
513 to temperature acclimation. J. Exp. Biol. 215, 1106–1116.
514 https://doi.org/10.1242/jeb.062273
515 Garland, M.A., Stillman, J.H., Tomanek, L., 2015. The proteomic response of cheliped myofibril tissue
516 in the eurythermal porcelain crab Petrolisthes cinctipes to heat shock following acclimation
517 to daily temperature fluctuations. J. Exp. Biol. 218, 388–403.
518 https://doi.org/10.1242/jeb.112250
519 Gavery, M.R., Nichols, K.M., Goetz, G.W., Middleton, M.A., Swanson, P., 2018. Characterization of
520 Genetic and Epigenetic Variation in Sperm and Red Blood Cells from Adult Hatchery and
521 Natural-Origin Steelhead, Oncorhynchus mykiss. G3 Bethesda Md 8, 3723–3736.
522 https://doi.org/10.1534/g3.118.200458
523 Jiang, L., Zhang, Jing, Wang, J.-J., Wang, L., Zhang, L., Li, G., Yang, X., Ma, X., Sun, X., Cai, J., Zhang,
524 Jun, Huang, X., Yu, M., Wang, X., Liu, F., Wu, C.-I., He, C., Zhang, B., Ci, W., Liu, J., 2013.
525 Sperm, but not oocyte, DNA methylome is inherited by zebrafish early embryos. Cell 153,
526 773–784. https://doi.org/10.1016/j.cell.2013.04.041
527 Kent, W.J., Zweig, A.S., Barber, G., Hinrichs, A.S., Karolchik, D., 2010. BigWig and BigBed: enabling
528 browsing of large distributed datasets. Bioinformatics 26, 2204–2207.
529 Kobayashi, H., Sakurai, T., Imai, M., Takahashi, N., Fukuda, A., Yayoi, O., Sato, S., Nakabayashi, K.,
530 Hata, K., Sotomaru, Y., Suzuki, Y., Kono, T., 2012. Contribution of intragenic DNA methylation
531 in mouse gametic DNA methylomes to establish oocyte-specific heritable marks. PLoS Genet.
532 8, e1002440. https://doi.org/10.1371/journal.pgen.1002440
533 Krueger, F., Andrews, S.R., 2011. Bismark: a flexible aligner and methylation caller for Bisulfite-Seq
534 applications. Bioinforma. Oxf. Engl. 27, 1571–1572.
535 https://doi.org/10.1093/bioinformatics/btr167
536 Krueger, F., Galore, T., n.d. A wrapper tool around Cutadapt and FastQC to consistently apply quality
537 and adapter trimming to FastQ files.
538 Lerer-Goldshtein, T., Bel, S., Shpungin, S., Pery, E., Motro, B., Goldstein, R.S., Bar-Sheshet, S.I.,
539 Breitbart, H., Nir, U., 2010. TMF/ARA160: A key regulator of sperm development. Dev. Biol.
540 348, 12–21. https://doi.org/10.1016/j.ydbio.2010.07.033
541 Lester, W.C., Johnson, T., Hale, B., Serra, N., Elgart, B., Wang, R., Geyer, C.B., Sperry, A.O., 2021.
542 Aurora A Kinase (AURKA) is required for male germline maintenance and regulates sperm
543 motility in the mouse. Biol. Reprod. 105, 1603–1616. https://doi.org/10.1093/biolre/ioab168
544 Liu, G., Wang, W., Hu, S., Wang, X., Zhang, Y., 2018. Inherited DNA methylation primes the
545 establishment of accessible chromatin during genome activation. Genome Res. 28, 998–
546 1007. https://doi.org/10.1101/gr.228833.117
547 Madeira, D., Araújo, J.E., Vitorino, R., Capelo, J.L., Vinagre, C., Diniz, M.S., 2016. Ocean warming alters
548 cellular metabolism and induces mortality in fish early life stages: A proteomic approach.
549 Environ. Res. 148, 164–176. https://doi.org/10.1016/j.envres.2016.03.030
550 Naud, N., Touré, A., Liu, J., Pineau, C., Morin, L., Dorseuil, O., Escalier, D., Chardin, P., Gacon, G., 2003.
551 Rho family GTPase Rnd2 interacts and co-localizes with MgcRacGAP in male germ cells.
552 Biochem. J. 372, 105–112. https://doi.org/10.1042/BJ20021652
553 Olia Bagheri, F., Alizadeh, A., Sadighi Gilani, M.A., Shahhoseini, M., 2021. Role of peroxisome
554 proliferator-activated receptor gamma (PPARγ) in the regulation of fatty acid metabolism

related gene expressions in testis of men with impaired spermatogenesis. Reprod. Biol. 21, 100543. https://doi.org/10.1016/j.repbio.2021.100543
Ortega-Recalde, O., Day, R.C., Gemmell, N.J., Hore, T.A., 2019. Zebrafish preserve global germline DNA methylation while sex-linked rDNA is amplified and demethylated during feminisation. Nat. Commun. 10, 3053. https://doi.org/10.1038/s41467-019-10894-7
Pepperl, J., Reim, G., Lüthi, U., Kaech, A., Hausmann, G., Basler, K., 2013. Sphingolipid depletion impairs endocytic traffic and inhibits Wingless signaling. Mech. Dev. 130, 493–505. https://doi.org/10.1016/j.mod.2013.04.001
Pires, E., Sung, P., Wiese, C., 2017. Role of RAD51AP1 in homologous recombination DNA repair and carcinogenesis. DNA Repair 59, 76–81. https://doi.org/10.1016/j.dnarep.2017.09.008
Potok, M.E., Nix, D.A., Parnell, T.J., Cairns, B.R., 2013. Reprogramming the maternal zebrafish genome after fertilization to match the paternal methylation pattern. Cell 153, 759–772. https://doi.org/10.1016/j.cell.2013.04.030
Robinson, J.T., Thorvaldsdóttir, H., Winckler, W., Guttman, M., Lander, E.S., Getz, G., Mesirov, J.P., 2011. Integrative genomics viewer. Nat Biotechnol 29, 24–26.
Shama, L.N.S., Wegner, K.M., 2014. Grandparental effects in marine sticklebacks: transgenerational plasticity across multiple generations. J. Evol. Biol. 27, 2297–2307. https://doi.org/10.1111/jeb.12490
Smit, P., AFA, Hubley, R.&. Green, 2015. RepeatMasker Open-4.0.
Sun, X., He, Y., Hou, L., Yang, W.-X., 2010. Myosin Va participates in acrosomal formation and nuclear morphogenesis during spermatogenesis of Chinese mitten crab Eriocheir sinensis. PloS One 5, e12738. https://doi.org/10.1371/journal.pone.0012738
Tani, M., Ito, M., Igarashi, Y., 2007. Ceramide/sphingosine/sphingosine 1-phosphate metabolism on the cell surface and in the extracellular space. Cell. Signal. 19, 229–237. https://doi.org/10.1016/j.cellsig.2006.07.001
Teymouri Zadeh, Z., Shariatmadari, F., Sharafi, M., Karimi Torshizi, M.A., 2020. Amelioration effects of n-3, n-6 sources of fatty acids and rosemary leaves powder on the semen parameters, reproductive hormones, and fatty acid analysis of sperm in aged Ross broiler breeder roosters. Poult. Sci. 99, 708–718. https://doi.org/10.1016/j.psj.2019.12.031
Tocher, D.R., Fonseca-Madrigal, J., Dick, J.R., Ng, W.-K., Bell, J.G., Campbell, P.J., 2004. Effects of water temperature and diets containing palm oil on fatty acid desaturation and oxidation in hepatocytes and intestinal enterocytes of rainbow trout (Oncorhynchus mykiss). Comp. Biochem. Physiol. B Biochem. Mol. Biol. 137, 49–63. https://doi.org/10.1016/j.cbpc.2003.10.002
Van Tran, L., Malla, B.A., Kumar, S., Tyagi, A.K., 2017. Polyunsaturated Fatty Acids in Male Ruminant Reproduction - A Review. Asian-Australas. J. Anim. Sci. 30, 622–637. https://doi.org/10.5713/ajas.15.1034
Velkova, M., Silva, N., Dello Stritto, M.R., Schleiffer, A., Barraud, P., Hartl, M., Jantsch, V., 2021. Caenorhabditis elegans RMI2 functional homolog-2 (RMIF-2) and RMI1 (RMH-1) have both overlapping and distinct meiotic functions within the BTR complex. PLoS Genet. 17, e1009663. https://doi.org/10.1371/journal.pgen.1009663
Wang, H., Wan, H., Li, X., Liu, W., Chen, Q., Wang, Y., Yang, L., Tang, H., Zhang, X., Duan, E., Zhao, X., Gao, F., Li, W., 2014. Atg7 is required for acrosome biogenesis during spermatogenesis in mice. Cell Res. 24, 852–869. https://doi.org/10.1038/cr.2014.70
White-Cooper, H., Bausek, N., 2010. Evolution and spermatogenesis. Philos. Trans. R. Soc. B Biol. Sci. 365, 1465–1480. https://doi.org/10.1098/rstb.2009.0323
Wu, H., Xu, T., Feng, H., Chen, L., Li, B., Yao, B., Qin, Z., Jin, P., Conneely, K.N., 2015. Detection of differentially methylated regions from whole-genome bisulfite sequencing data without replicates. Nucleic Acids Res 43, e141.
Yefimova, M.G., Buschiazzo, A., Burel, A., Lavault, M.-T., Pimentel, C., Jouve, G., Jaillard, S., Jegou, B., Bourmeyster, N., Ravel, C., 2019. Autophagy is increased in cryptorchid testis resulting in abnormal spermatozoa. Asian J. Androl. 21, 570–576. https://doi.org/10.4103/aja.aja_12_19

Young, M.M., Wang, H.-G., 2018. Sphingolipids as Regulators of Autophagy and Endocytic Trafficking. Adv. Cancer Res. 140, 27–60. https://doi.org/10.1016/bs.acr.2018.04.008
Zakrzewski, P., Rędowicz, M.J., Buss, F., Lenartowska, M., 2020. Loss of myosin VI expression affects acrosome/acroplaxome complex morphology during mouse spermiogenesis†. Biol. Reprod. 103, 521–533. https://doi.org/10.1093/biolre/ioaa071
Zhao, J., Liu, T., Jin, S., Wang, X., Qu, M., Uhlén, P., Tomilin, N., Shupliakov, O., Lendahl, U., Nistér, M., 2011. Human MIEF1 recruits Drp1 to mitochondrial outer membranes and promotes mitochondrial fusion rather than fission. EMBO J. 30, 2762–2778. https://doi.org/10.1038/emboj.2011.198

						Nuclear					Mitochondrial	
Tissue	Fish	Total raw reads	Trimmed reads	% of mapping	BS conversion (%)	Average CpG sequencing depth (x)	% CpGs covered 1x	% CpGs covered 5x	% CpGs covered 10x	CpG methylation (%)	Average CpG sequencing depth (x)	CpG methylation (%)
Muscle 12°C	1	324 054 890	312 036 061	60,16	99,35	11,02	93,38	78,93	54,04	78,13	2152,99	1,03
	2	314 187 112	301 636 081	58,86	99,38	10,46	92,47	77,44	50,38	74,80	2122,71	0,95
	3	323 609 587	313 382 478	60,34	99,36	11,24	92,59	78,67	54,56	74,47	2534,55	0,78
	4	346 904 275	334 318 944	60,55	99,37	12,05	93,06	79,82	58,62	75,70	3314,62	0,75
				59,98	99,37	11,19	92,88	78,71	54,40	75,77	2531,22	0,88
Sperm 12°C	1	300 587 067	294 303 143	59,66	99,15	10,58	92,29	77,88	50,85	88,41	74,09	7,65
	2	325 691 293	321 065 565	61,02	99,42	11	92,52	78,78	54,54	88,32	77,54	6,98
	3	336 626 182	332 307 052	61,31	99,39	11,54	92,57	79,35	56,11	88,47	62,51	5,23
	4	309 900 540	305 834 179	46,18	99,48	8,97	92,11	71,22	37,33	88,74	75,62	5,66
	5	332 585 217	326 170 573	59,67	99,50	11,07	92,76	78,98	54,21	88,25	39,75	11,90
	6	306 207 661	301 165 523	60,48	99,38	10,68	92,29	77,88	50,85	88,49	29,34	9,80
				58,05	99,39	10,64	92,43	76,81	49,71	88,45	59,81	7,87
Sperm 16°C	7	340 298 820	335 329 836	61,66	99,39	11,14	92,77	79,58	56,22	88,43	34,56	15,56
	8	309 013 645	304 553 951	60,67	99,40	10,71	92,71	78,56	52,32	88,71	113,23	5,21
	9	313 593 505	307 126 184	60,35	99,34	10,81	92,68	78,64	52,58	88,46	123,90	4,62
	10	311 388 841	305 315 136	61,97	99,35	11,17	92,51	78,71	54,59	88,77	76,70	4,12
	11	336 389 118	330 578 540	60,27	99,40	11,37	92,64	79,30	55,42	88,62	74,01	7,00
	12	311 912 118	306 606 582	60,73	99,36	11,03	92,59	78,91	54,24	88,61	54,91	5,06
				60,94	99,37	11,04	92,65	78,95	54,23	88,60	79,55	6,93

Tab 1. Summary of WGBS

Paired reads were mapped uniquely to the rainbow trout genome (Omik_1.0) using Bismark. Average sequencing depth. indicates the mean number of reads per position in nuclear and mitochondrial genomes.
The nuclear coverage represents the proportion of mapped CpGs over the total number of CpG sites in the nuclear genome, here calculated under 1X, 5X or 10X sequencing depth selection threshold.

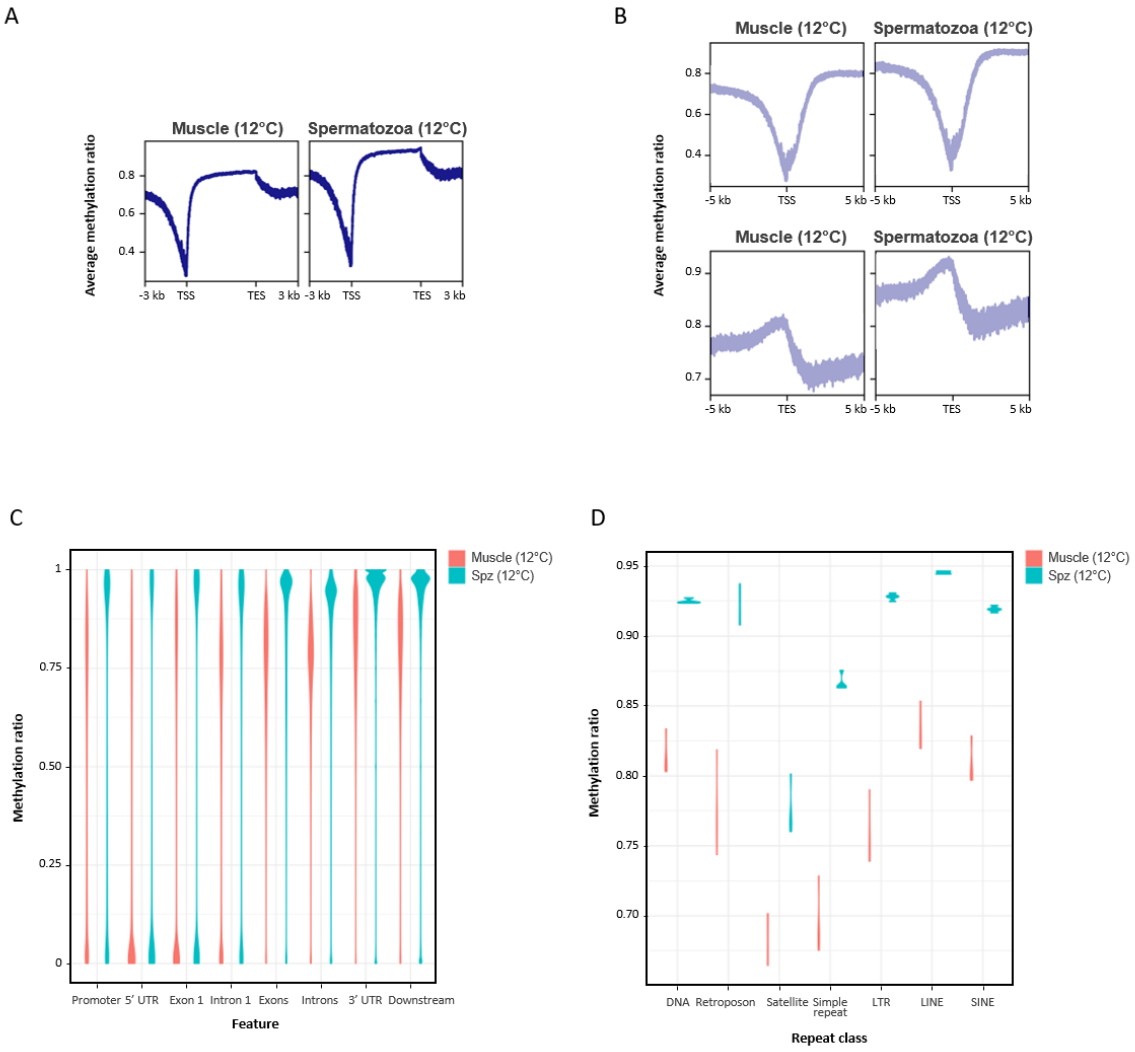

Fig 1. Global DNA methylation in rainbow trout control muscle and spermatozoa according to genomic features

A. Average methylation profiles along the 115 853 annotated ensembl coding and non-coding transcripts of ensembl v104 Omyk_1.0 genome. B. Average methylation profiles around TSS (+/- 5 kb) (left panels) and TES (+/- 5 kb) (right panels). C. Distribution of methylation ratios according to gene features: promoter regions (-1 kb ; TSS), 5'UTR, exon1, intron1, all exons, all introns, 3'UTR and downstream regions (TES ; +1 kb). D. Distribution of methylation ratios found in muscle and sperm in transposons (DNA), retroposons, satellites, simple repeats, LTR containing elements, LINEs and SINEs.

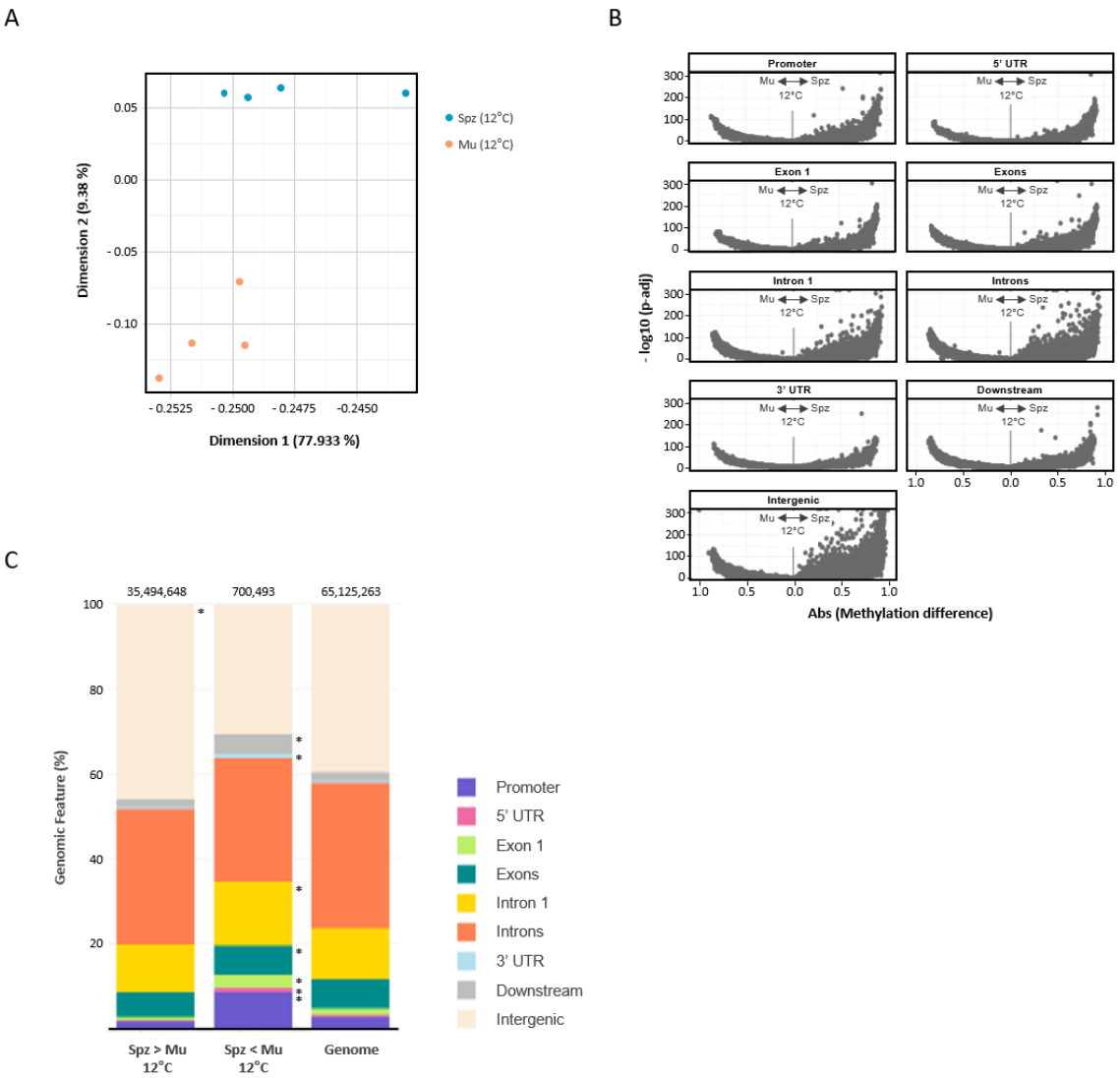

Fig 2. Differentially methylated cytosines between control spermatozoa and muscle

A. PCA plot of spermatozoa and muscle WGBS data sets. B. Volcano plots of DMCs between spermatozoa and muscle in every genomic feature (x axis : absolute methylation difference, y : -log10 (adusted p-value)). C. Relative distributions of DMCs (Spz > Mu : hypermethylated in sperm compared to muscle; Spz < Mu : hypomethylated in sperm compared to muscle) according to genome features (promoter regions (-1 kb ; TSS), 5'UTR, exon1, intron1, all exons, all introns, 3'UTR, downstream (TES ; +1 kb) and intergenic regions). The reference set (Genome) contains all analyzed CpGs. Genome features statistically enriched in DMCs compared to the reference set are indicated with an * (binomial test).

670

A

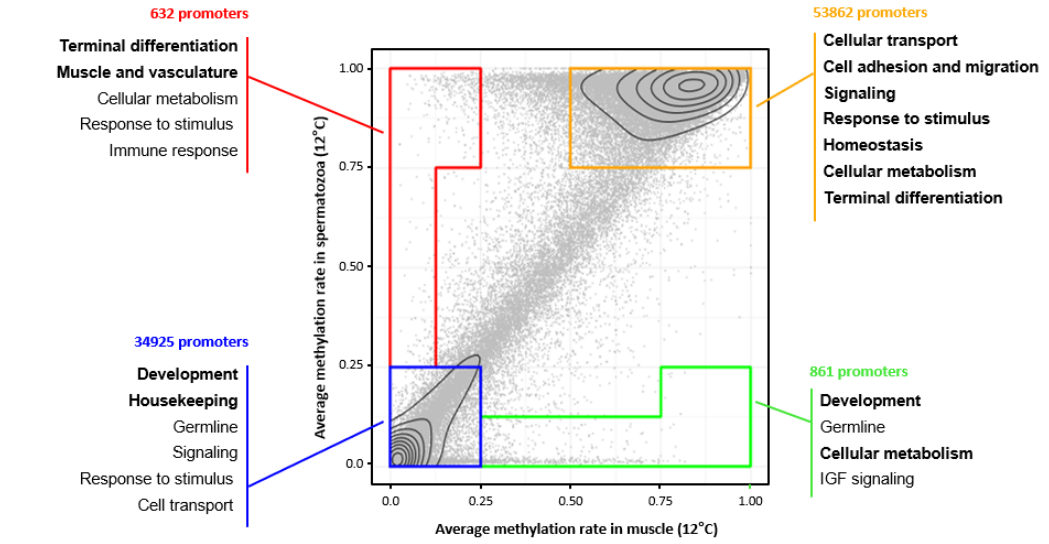
632 promoters
Terminal differentiation
Muscle and vasculature
Cellular metabolism
Response to stimulus
Immune response
53862 promoters
Cellular transport
Cell adhesion and migration
Signaling
Response to stimulus
Homeostasis
Cellular metabolism
Terminal differentiation
34925 promoters
Development
Housekeeping
Germline
Signaling
Response to stimulus
Cell transport
861 promoters
Development
Germline
Cellular metabolism
IGF signaling
Average methylation rate in spermatozoa (12°C)
Average methylation rate in muscle (12°C)
0.0
0.25
0.50
0.75
1.00

B

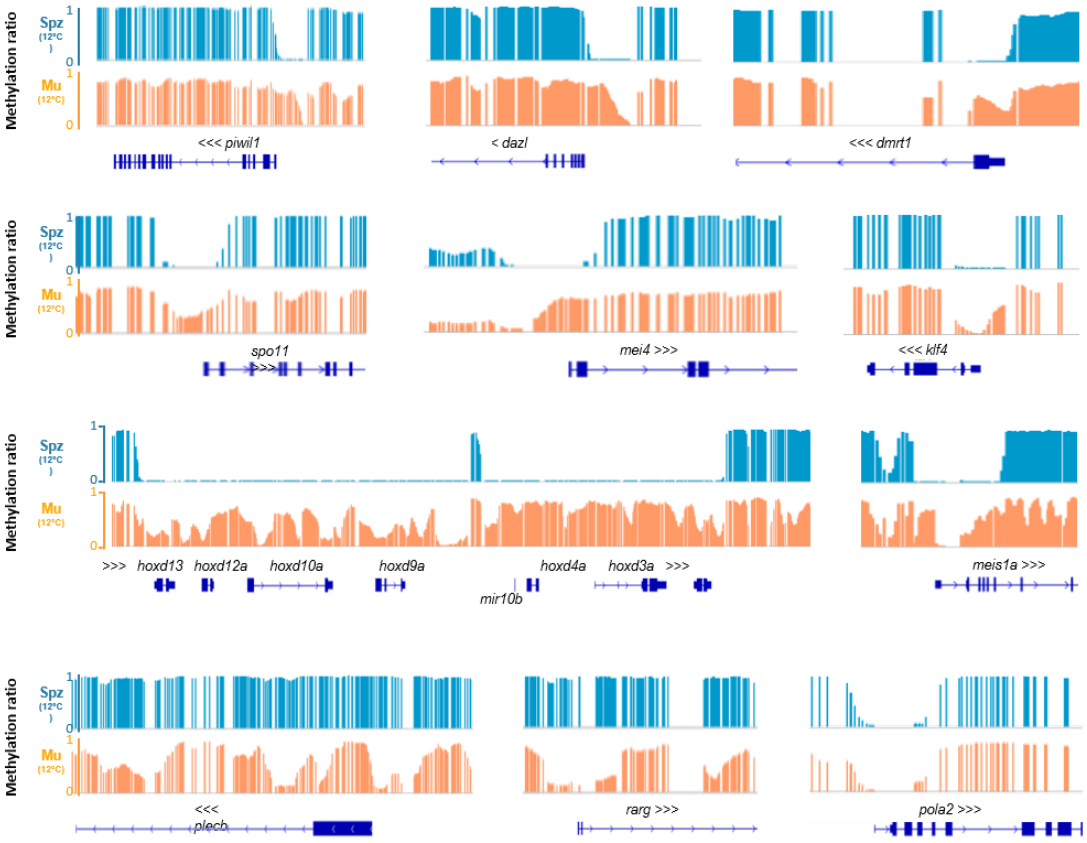
Methylation ratio
Spz (12°C)
Mu (12°C)
<<< piwil1
< dazl
<<< dmrt1
spo11 >>>
mei4 >>>
<<< klf4
>>> hoxd13 hoxd12a hoxd10a hoxd9a
hoxd4a hoxd3a >>>
mir10b
meis1a >>>
<<< plecb
rarg >>>
pola2 >>>

671

Fig 3. Differentially methylated gene promoters between control spermatozoa and muscle

A. Plot of average methylation of ensembl omyk_1.0 v105 transcrits promoters in muscle (x axis) *versus* spermatozoa (y axis). Common hypo-methylated promoters are highlighted in the blue square, common hyper-methylated promoters in the orange shape, muscle-specific hypo-methylated promoters in the red shape and spermatozoa-specific promoters in the green shape. Functional annotation terms deduced from a GO term enrichment analysis and corresponding to each class are indicated. B. IGB snapshots of transcripts or TSS regions as examples of spermatozoa-specific hypo-methylated promoters (*piwil1*, *dazl*, *dmrt1*, *spo11*, *mei4*, *hox* cluster and *mir10b*, *meis1a*), muscle-specific hypo-methylated promoters (*plecb* and *rarg*) or common hypo-methylated promoter (*pola2*). Muscle : Mu; Spermatozoa : Spz.

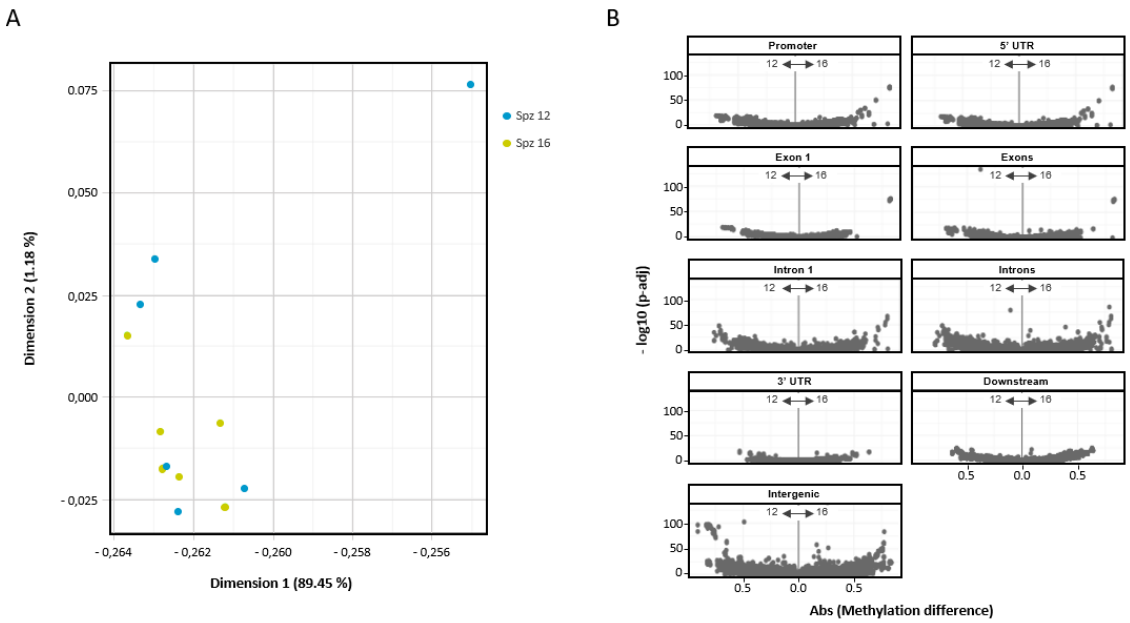

Fig 4. Differentially methylated cytosines between spermatozoa from males raised at 16°C versus 12°C

A. PCA plot of spermatozoa from males raised at 12°C and 16°C WGBS data sets. B. Volcano plots of DMCs between spermatozoa from males raised at 12°C versus 16°C in every genomic feature (x axis : absolute methylation difference, y : -log10 (adusted p-value)).

716

A

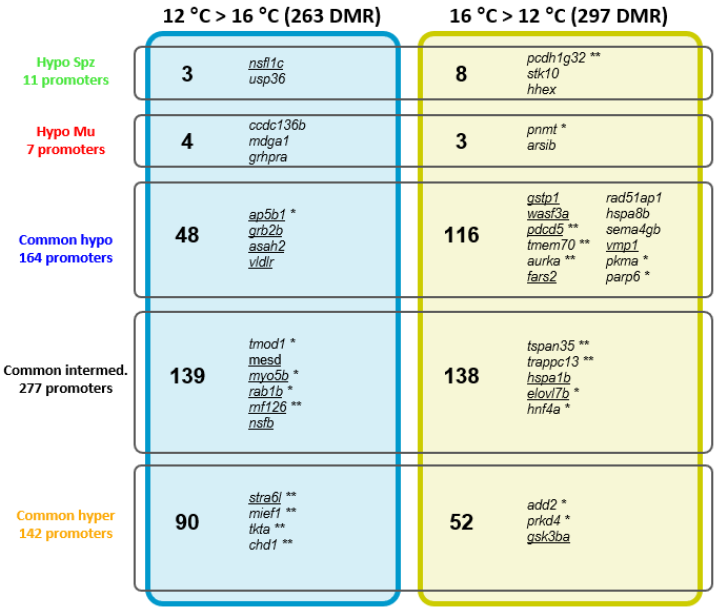

12 °C > 16 °C (263 DMR)

Cellular lipid catabolic process
Leukotriene metabolic process
Vesicle-mediated transport
Nuclear membrane reassembly
Autophagosome assembly
Positive regulation of PPAR signaling
Pseudohyphal growth

16 °C > 12 °C (297 DMR)

Long-chain fatty acid metabolic process
Prostaglandin metabolic process
Phenylalanyl-tRNA aminoacylation
Calcium ion transmembrane transport
Intracellular lipid transport
Axonal fasciculation
Microtubule anchoring at centrosome
Negative regulation of JUN kinase activity
Chaperone-mediated protein folding

B

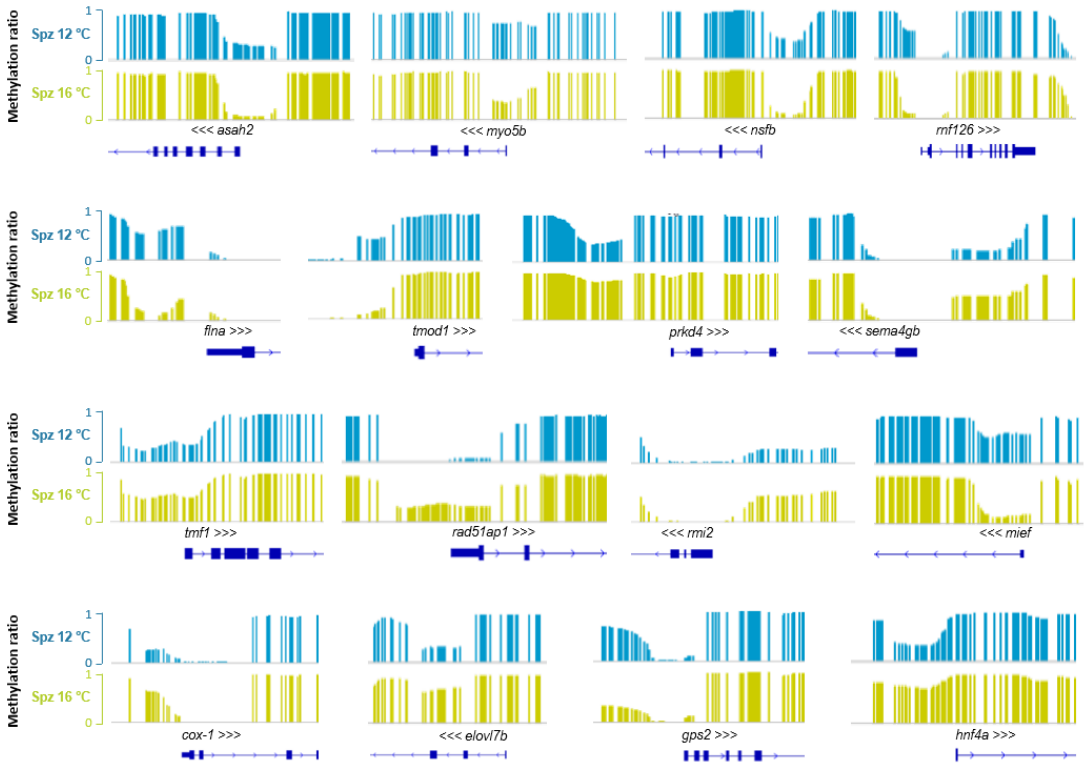

717

718

Fig 5: Differentially methylated gene promoters between spermatozoa of fish raised at 16°C *versus* 12°C

A. Intersection of up- and down-regulated DMRs with the different promoter categories defined in Fig 3 (sperm-specific hyper or hypo-methylated, equally methylated,…) and associated GO term enrichment analysis. Genes are given of examples of each categories, chosen either for their association to an enriched GO term or for their presence in the top200 list of prom-DMRs. underlined: associated to an enriched GO terms,*: top 10, **: top 50 prom-DMR. B. IGV snapshots of TSS regions as examples of hyper- and hypo-methylated promoters at 16°C versus 12°C.

A

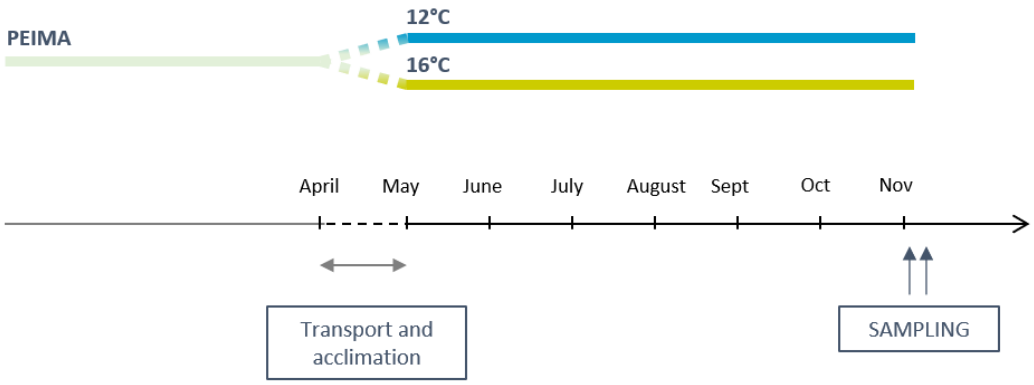

B

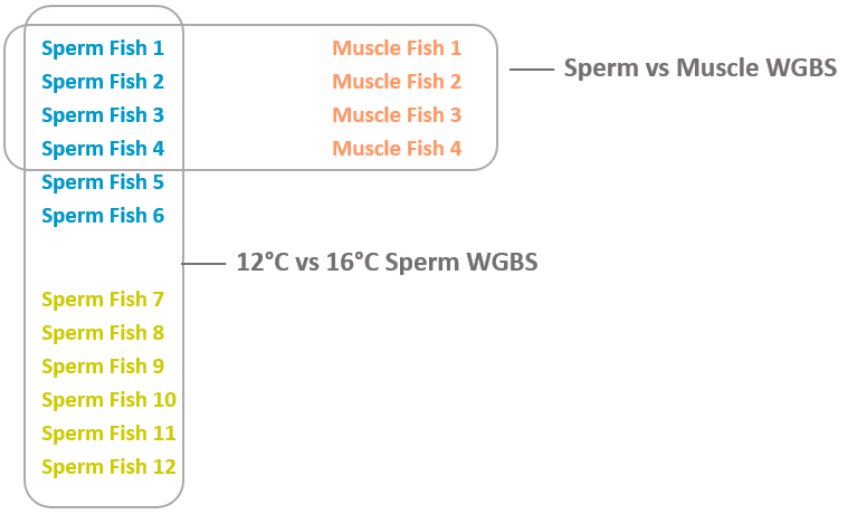

746

747

748 **Suppl Fig 1. Experimental design**

749 A. *Oncorhynchus mykiss* rainbow trouts were reared in our experimental farm and transferred to our
750 indoor fish facility in April of their second year. Two groups of 20 males were kept in a recycling
751 system, under artificial spring/summer/autumn photoperiod, and at the temperatures of 12°C and
752 16°C (after 2 weeks acclimation and gradual temperature increase). Fish sperm and muscle were
753 sampled during the reproduction period. B. Four fish were sequenced for the sperm versus muscle
754 paired analysis while two groups of 6 fish were sequenced for the study of the temperature contrast
755 in spermatozoa.

756

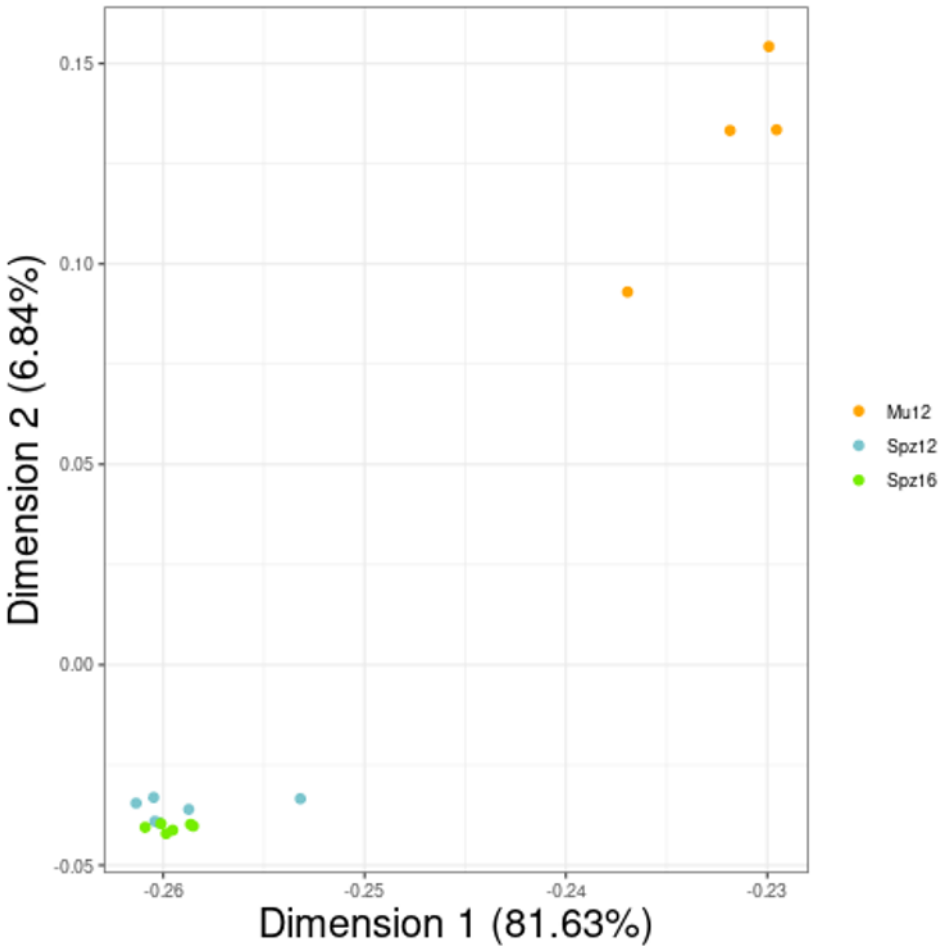

Suppl Fig 2. PCA plot of muscle (Mu12), spermatozoa from males raised at 12°C (Spz12) and spermatozoa from males raised at 16°C (Spz16) WGBS data sets

PRDM9 p-val 9.28e-35

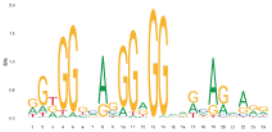

Suppl Fig 3. Putative recombination hotspots enrichment in DMRs between spermatozoa from males raised at 16°C versus 12°C.

Vertebrate PRDM9 consensus DNA binding site identified by MEME in DMR sequences between spermatozoa from males raised at 16°C versus 12°C, and associated p-vamue.

MEME suite is accessible online (https://meme-suite.org/meme/), SEA algorithm was used.

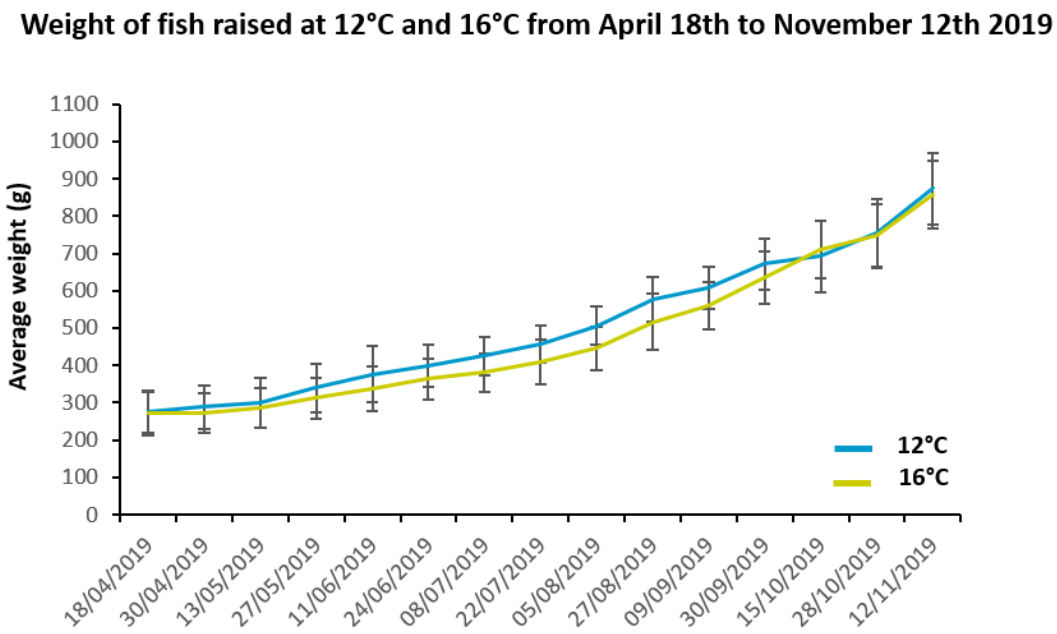

789

790

791 **Suppl Fig 4. Evolution of the weight of the fish raised at 12°C and 16° during the exposure to the**
792 **temperature increase.**

793 Fish weight was individualy recorded every 2 weeks. The graph shows the weight averages and
794 standard deviations found for each group between April 18 and November 12 2019.

795